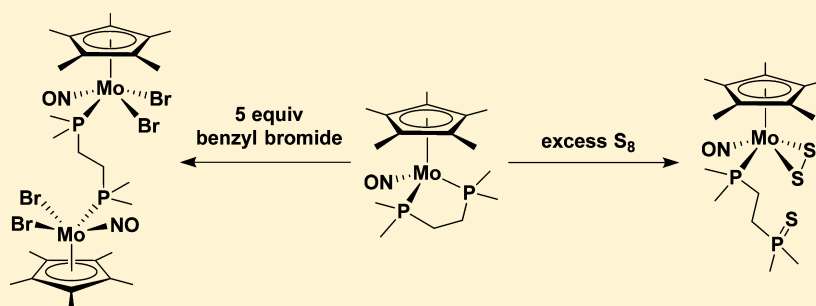


Hemilability of the 1,2-Bis(dimethylphosphino)ethane (dmpe) Ligand in Cp*Mo(NO)(κ^2 -dmpe)Aaron S. Holmes, Brian O. Patrick, Taleah M. Levesque, and Peter Legzdins*^{ID}

Department of Chemistry, The University of British Columbia, Vancouver, British Columbia V6T 1Z1, Canada

S Supporting Information



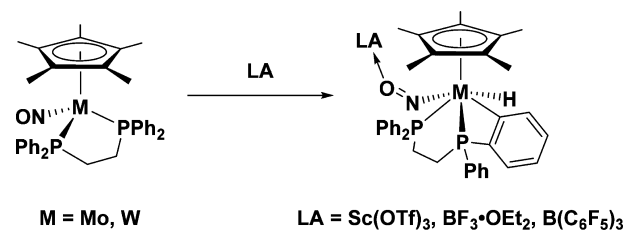
ABSTRACT: Reaction of Cp*Mo(NO)Cl₂ with 1 equiv of 1,2-bis(dimethylphosphino)ethane (dmpe) in THF at ambient temperature forms [Cp*Mo(NO)(Cl)(κ^2 -dmpe)]Cl (1), which is isolable as an analytically pure yellow powder in 65% yield. Further addition of 2 equiv of Cp₂Co to 1 in CH₂Cl₂ affords dark red Cp*Mo(NO)(κ^2 -dmpe) (2), which was isolated in 36% yield by recrystallization from Et₂O at -30 °C. Reaction of a benzene solution of 2 with an equimolar amount of elemental sulfur results in the immediate production of dark blue (μ -S)[Cp*Mo(NO)(κ^1 -dmpeS)]₂ (3), which is a rare example of a bimetallic transition-metal complex bridged by only a single sulfur atom and involving Mo=S=Mo bonding. In contrast, reaction of 2 with an excess of sulfur in benzene results in the formation of Cp*Mo(NO)(η^2 -S₂)(κ^1 -dmpeS) (4). Complex 4 can also be formed by the addition of elemental sulfur to 3, thereby indicating that 3 is a precursor to 4. Cp*Mo(NO)(κ^2 -dmpe) (2) also undergoes interesting transformations when treated with organic bromides. For instance, reaction of 2 with 5 equiv benzyl bromide in THF produces the bimetallic complex (μ -dmpe)[Cp*Mo(NO)Br₂]₂ (5) and bibenzyl after 4 d at 70 °C probably via radical intermediates. In contrast to its reaction with benzyl bromide, complex 2 forms [Mo(NO)Br₂(κ^2 -dmpe)]₂ (6), olefin, alkane, and Cp*H when treated with 5 equiv of 1-bromopropane or 1-bromooctane in THF at 70 °C for 72 h. Interestingly, complex 2 does not display any reactivity with bromobenzene or 1-bromoadamantane even after being heated for several days at 70 °C. All new complexes were characterized by conventional spectroscopic and analytical methods, and the solid-state molecular structures of most of them were established by single-crystal X-ray crystallographic analyses.

INTRODUCTION

We previously developed Cp*M(NO)-containing complexes (Cp* = η^5 -C₅Me₅; M = Mo or W) as reagents for the selective activation and functionalization of unreactive hydrocarbon C-H bonds.^{1,2} We recently extended our investigations to compounds that possess electron-rich metal centers such as Cp*M(NO)(κ^2 -dppe) (dppe = Ph₂PCH₂CH₂PPh₂) that should, in principle, facilitate the oxidative addition of hydrocarbon C-H bonds to them. Interestingly, the Cp*M(NO)(κ^2 -dppe) compounds are rendered prone to effecting C-H activation reactions not by thermolyses but rather by treatment with equimolar amounts of appropriate Lewis acids (LA) which form adducts with the basic O-termini of their nitrosyl ligands (Scheme 1).³

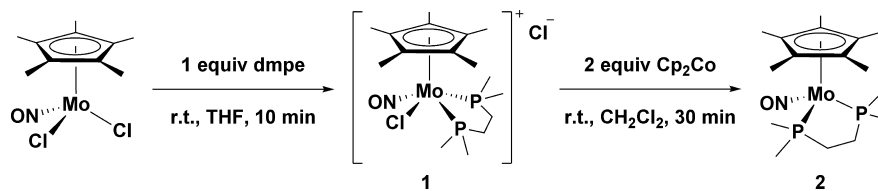
Regrettably, these systems only promote intramolecular C-H activations, presumably because steric factors in the metal's coordination sphere bring one of the phenyl substituents of the dppe ligand into a position in which it can readily undergo *ortho*-metalation. To overcome this mode of reactivity, we then focused our attention on the related but less sterically

Scheme 1. Lewis-Acid Induced Intramolecular C-H Activation



encumbered Cp*M(NO)(κ^2 -dmpe) (dmpe = 1,2-bis(dimethylphosphino)ethane, Me₂PCH₂CH₂PMe₂) complexes. Regrettably, treatment of the dmpe compounds with Lewis acids does not result in the desired intermolecular C-H activations.⁴ Consequently, we extended our investigations to

Received: July 7, 2017

Scheme 2. Two-Step Preparation of $\text{Cp}^*\text{Mo}(\text{NO})(\kappa^2\text{-dmpe})$ 

encompass other reactants to establish the characteristic chemical properties of the $\text{Cp}^*\text{M}(\text{NO})(\kappa^2\text{-dmpe})$ complexes. In this article, we report on the novel reactions of one of them, namely $\text{Cp}^*\text{Mo}(\text{NO})(\kappa^2\text{-dmpe})$, with elemental sulfur and organic halides. These reactants were chosen for initial examination because they are known to exhibit a variety of different reaction modes with transition-metal complexes.

RESULTS AND DISCUSSION

Two-Step Preparation of $\text{Cp}^*\text{Mo}(\text{NO})(\kappa^2\text{-dmpe})$.

Step 1: As summarized in Scheme 2, treatment of a green THF solution of $\text{Cp}^*\text{Mo}(\text{NO})\text{Cl}_2$ with 1 equiv of dmpe at ambient temperatures results in a ligand-substitution reaction and the production of $[\text{Cp}^*\text{Mo}(\text{NO})(\kappa^2\text{-dmpe})\text{Cl}]\text{Cl}$ (**1**), which can be isolated as a yellow powder in 65% yield. Recrystallization of this powder from CH_2Cl_2 /hexanes at room temperature affords single crystals of the salt as a dihydrate that were subjected to an X-ray diffraction analysis. The crystal structure of **1**·2H₂O consists of the packing of discrete cations and anions along with the two water molecules with the solid-state molecular structure of the cation (shown in Figure 1) being that of a four-legged piano-stool having metrical parameters similar to those

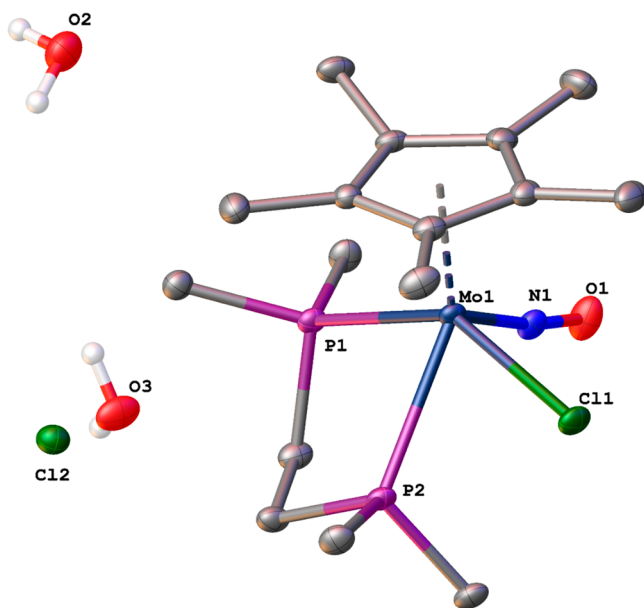


Figure 1. Solid-state molecular structure of $[\text{Cp}^*\text{Mo}(\text{NO})(\kappa^2\text{-dmpe})\text{Cl}]\text{Cl}$ (**1**) as its dihydrate with 50% probability thermal ellipsoids shown. Most hydrogen atoms were omitted for the sake of clarity. Selected bond lengths (Å) and angles (deg): $\text{Mo}(1)\text{-P}(1) = 2.5447(5)$, $\text{Mo}(1)\text{-P}(2) = 2.5537(5)$, $\text{Mo}(1)\text{-Cl}(1) = 2.4785(5)$, $\text{Mo}(1)\text{-N}(1) = 1.7889(18)$, $\text{N}(1)\text{-O}(1) = 1.201(2)$, $\text{Mo}(1)\text{-N}(1)\text{-O}(1) = 171.82(16)$, $\text{P}(1)\text{-Mo}(1)\text{-P}(2) = 74.840(17)$, $\text{P}(2)\text{-Mo}(1)\text{-Cl}(1) = 72.186(16)$, $\text{Cl}(1)\text{-Mo}(1)\text{-N}(1) = 91.76(6)$, $\text{N}(1)\text{-Mo}(1)\text{-P}(1) = 80.89(5)$.

exhibited by related species.⁶ The spectroscopic properties of **1** are fully consistent with the $[\text{Cp}^*\text{Mo}(\text{NO})(\kappa^2\text{-dmpe})\text{Cl}]^+$ cation retaining this structure in solution. Thus, the ¹H NMR spectrum of **1** in CD_2Cl_2 (Figure S1) exhibits signals due to four inequivalent methyl and methylene groups and a singlet at δ 2.00 ppm corresponding to the Cp* ligand. Consistently, its ³¹P{¹H} NMR spectrum in the same solvent (Figure S3) shows two doublets at δ 37.4 and 44.9 ppm with ²J_{PP} = 45.6 Hz.

Step 2: Reduction of $[\text{Cp}^*\text{Mo}(\text{NO})(\kappa^2\text{-dmpe})\text{Cl}]\text{Cl}$ (**1**) with 2 equiv of Cp_2Co affords dark red $\text{Cp}^*\text{Mo}(\text{NO})(\kappa^2\text{-dmpe})$ (**2**) which was isolated as an analytically pure solid in 36% overall yield from $\text{Cp}^*\text{Mo}(\text{NO})\text{Cl}_2$ by recrystallization from Et_2O at -30 °C. The ¹H, ¹³C{¹H}, and ³¹P{¹H} NMR spectra of **2** in C_6D_6 solutions confirm the three-legged piano-stool molecular structure shown for the complex in Scheme 2. For instance, its ¹H NMR spectrum in C_6D_6 (Figure S5) shows two sets of doublets that belong to two of the P(CH₃)₃ groups that are directed toward and two away from the Cp* ring. As expected, the ³¹P{¹H} NMR spectrum (Figure S7) shows a singlet at δ 57.1 ppm. The IR spectrum of **2** exhibits a strong $\nu(\text{NO})$ absorption at 1535 cm^{-1} , which is a manifestation of the significant electron density extant at the Mo(0) center that results in turn in considerable Mo → NO backbonding. The solid-state molecular structure of **2** was confirmed by a single-crystal X-ray diffraction analysis and is shown in Figure 2. As expected, its metrical parameters are similar to those exhibited by $\text{Cp}^*\text{Mo}(\text{NO})(\kappa^2\text{-dppe})$.³

The presence of the electron-rich metal center in $\text{Cp}^*\text{Mo}(\text{NO})(\kappa^2\text{-dmpe})$ led us to investigate its reactivity with typical oxidants such as elemental sulfur and alkyl bromides to delineate its characteristic chemical properties. The reactions with sulfur are described first.

Reaction of $\text{Cp}^*\text{Mo}(\text{NO})(\kappa^2\text{-dmpe})$ with 1/8 S₈: Preparation of $(\mu\text{-S})[\text{Cp}^*\text{Mo}(\text{NO})(\kappa^1\text{-dmpeS})]_2$ (3**).** As summarized in Scheme 3, reaction of a benzene solution of $\text{Cp}^*\text{Mo}(\text{NO})(\kappa^2\text{-dmpe})$ with an equimolar amount of elemental sulfur results in an oxidation reaction and the immediate production of the Mo(II) complex, $(\mu\text{-S})[\text{Cp}^*\text{Mo}(\text{NO})(\kappa^1\text{-dmpeS})]_2$ (**3**), which was isolated as a dark blue solid in 48% yield following column chromatography on basic alumina. Approximately one-half of the initial reactant **2** can be recovered from the final reaction mixture, thereby indicating that the formation of **3**, a 3:2 S:Mo bimetallic complex, is favored over that of other molybdenum complexes incorporating one or two sulfur atoms per metal center. The solid-state molecular structure of **3** is shown in Figure 3, and it confirms that one phosphorus end of the dmpe ligand in **2** was displaced from the molybdenum's coordination sphere and converted into a phosphine sulfide. In addition, the resulting 16e $\text{Cp}^*\text{Mo}(\text{NO})(\kappa^1\text{-dmpeS})$ fragment is linked to another of its kind by a Mo=S=Mo bridge that allows each metal center to attain the favored 18e configuration.⁷ The molybdenum-sulfur bond length of $2.2965(4)$ Å is intermediate between those reported for Mo=S ($\sim 2.10\text{-}2.20$ Å) and Mo-S ($\sim 2.35\text{-}2.45$

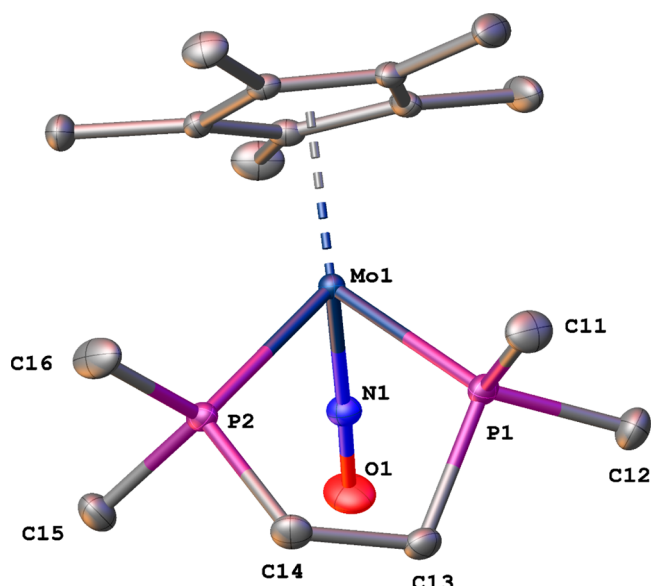
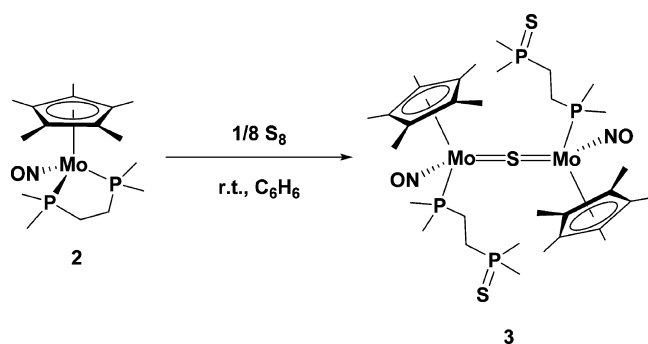


Figure 2. Solid-state molecular structure of $\text{Cp}^*\text{Mo}(\text{NO})(\kappa^2\text{-dmpe})$ (**2**) with 50% probability thermal ellipsoids shown. Hydrogen atoms were omitted for the sake of clarity. Selected bond lengths (Å) and angles (deg): $\text{Mo}(1)\text{-P}(1) = 2.3884(4)$, $\text{Mo}(1)\text{-P}(2) = 2.3866(4)$, $\text{Mo}(1)\text{-N}(1) = 1.7864(11)$, $\text{N}(1)\text{-O}(1) = 1.2243(14)$, $\text{P}(1)\text{-C}(11) = 1.8284(14)$, $\text{P}(1)\text{-C}(12) = 1.8270(14)$, $\text{P}(1)\text{-C}(13) = 1.8439(14)$, $\text{P}(2)\text{-C}(14) = 1.8556(13)$, $\text{P}(2)\text{-C}(15) = 1.8217(14)$, $\text{P}(2)\text{-C}(16) = 1.8287(14)$, $\text{C}(13)\text{-C}(14) = 1.5288(19)$, $\text{Mo}(1)\text{-N}(1)\text{-O}(1) = 177.33(11)$, $\text{N}(1)\text{-Mo}(1)\text{-P}(1) = 87.45(4)$, $\text{N}(1)\text{-Mo}(1)\text{-P}(2) = 87.31(4)$, $\text{P}(1)\text{-Mo}(1)\text{-P}(2) = 79.813(13)$.

Scheme 3. Reaction of $\text{Cp}^*\text{Mo}(\text{NO})(\kappa^2\text{-dmpe})$ with an Equimolar Amount of S_8



Å) linkages,^{8–11} and there is no Mo–Mo bond because the separation of 4.4559(10) Å precludes a significant interaction between the metal centers.^{11,12} In addition, the P=S distance of 1.9647(12) Å is as expected for such a bond.¹³ In the solid state, the two halves of **3** are crystallographically equivalent, and the molecule belongs to the C_2 point group (Figure 3).

The spectroscopic properties of **3** in solutions are completely consistent with the molecular structure depicted in Figure 3. Thus, its ^1H and $^{31}\text{P}\{^1\text{H}\}$ NMR spectra in C_6D_6 (Figures S8 and S10, respectively) exhibit signals resulting from the two different PMe_2 and CH_2 environments. In addition, the nitrosyl-stretching frequency of 1562 cm^{-1} in its IR spectrum again indicates the presence of significant electron density at the two molybdenum centers.

Reaction of $\text{Cp}^*\text{Mo}(\text{NO})(\kappa^2\text{-dmpe})$ with an Excess of S_8 : Preparation of $\text{Cp}^*\text{Mo}(\text{NO})(\eta^2\text{-S}_2)(\kappa^1\text{-dmpeS})$ (4**).** Exposure of a benzene solution of $\text{Cp}^*\text{Mo}(\text{NO})(\kappa^2\text{-dmpe})$ to

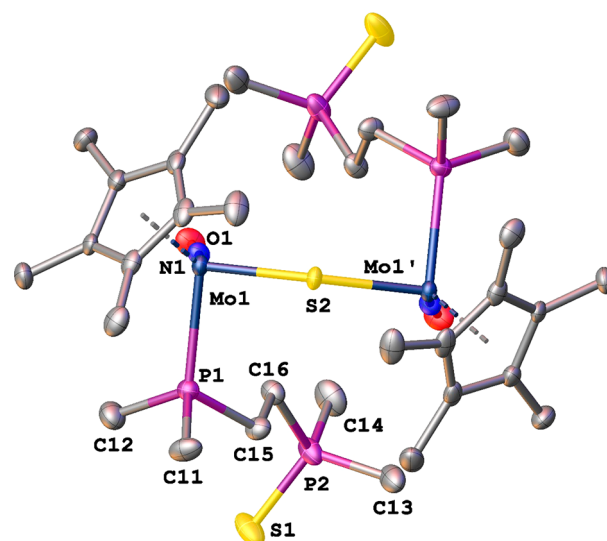


Figure 3. Solid-state molecular structure of $(\mu\text{-S})[\text{Cp}^*\text{Mo}(\text{NO})(\kappa^1\text{-dmpeS})]_2$ (**3**) with 50% probability thermal ellipsoids shown. Hydrogen atoms were omitted for the sake of clarity. Only one-half of the bimetallic molecule was fully labeled for the sake of clarity because the two halves are symmetry related. Selected bond lengths (Å) and angles (deg): $\text{Mo}(1)\text{-S}(2) = 2.2965(4)$, $\text{Mo}(1)\text{-P}(1) = 2.4550(8)$, $\text{Mo}(1)\text{-N}(1) = 1.781(3)$, $\text{N}(1)\text{-O}(1) = 1.226(3)$, $\text{P}(1)\text{-C}(11) = 1.820(3)$, $\text{P}(1)\text{-C}(12) = 1.827(4)$, $\text{P}(1)\text{-C}(15) = 1.832(3)$, $\text{P}(2)\text{-C}(13) = 1.793(4)$, $\text{P}(2)\text{-C}(14) = 1.798(4)$, $\text{P}(2)\text{-C}(16) = 1.816(3)$, $\text{P}(2)\text{-S}(1) = 1.9647(12)$, $\text{C}(15)\text{-C}(16) = 1.531(4)$, $\text{Mo}(1)\text{-N}(1)\text{-O}(1) = 172.6(3)$, $\text{S}(2)\text{-Mo}(1)\text{-P}(1) = 91.57(2)$, $\text{P}(1)\text{-Mo}(1)\text{-N}(1) = 87.98(8)$, $\text{N}(1)\text{-Mo}(1)\text{-S}(2) = 105.68(9)$, $\text{Mo}(1)\text{-S}(2)\text{-Mo}(1') = 151.93(5)$.

an excess of elemental sulfur affords the novel Mo(II) complex $\text{Cp}^*\text{Mo}(\text{NO})(\eta^2\text{-S}_2)(\kappa^1\text{-dmpeS})$ (**4**), which can be isolated in reasonable yields as a red solid following column chromatography on basic alumina (Scheme 4). The ^1H and $^{31}\text{P}\{^1\text{H}\}$ NMR spectroscopic properties of C_6D_6 solutions of **4** (Figures S12 and S14) are fully consistent with it possessing the monomeric structure shown in Scheme 4.

Scheme 4. Reaction of $\text{Cp}^*\text{Mo}(\text{NO})(\kappa^2\text{-dmpe})$ with an Excess of S_8



Small red crystals of **4** suitable for an X-ray diffraction analysis were obtained by vapor diffusion of Et_2O into a C_6H_6 solution of the complex over 3 d in an inert atmosphere at room temperature. The solid-state molecular structure of **4** is that of a four-legged piano stool (Figure 4). The $\text{Mo}(1)\text{-S}(1)$ and $\text{Mo}(1)\text{-S}(2)$ linkages are both single bonds, as indicated by their bond lengths of 2.450(5) and 2.459(4) Å, respectively, and the $\text{S}(1)\text{-S}(2)$ linkage in the $\eta^2\text{-S}_2$ ligand has a bond length of 2.059(4) Å, as expected for a S–S single bond.^{14,15} Finally, complex **4** has a $\text{Mo}(1)\text{-P}(1)$ bond length of 2.4696(13) Å,

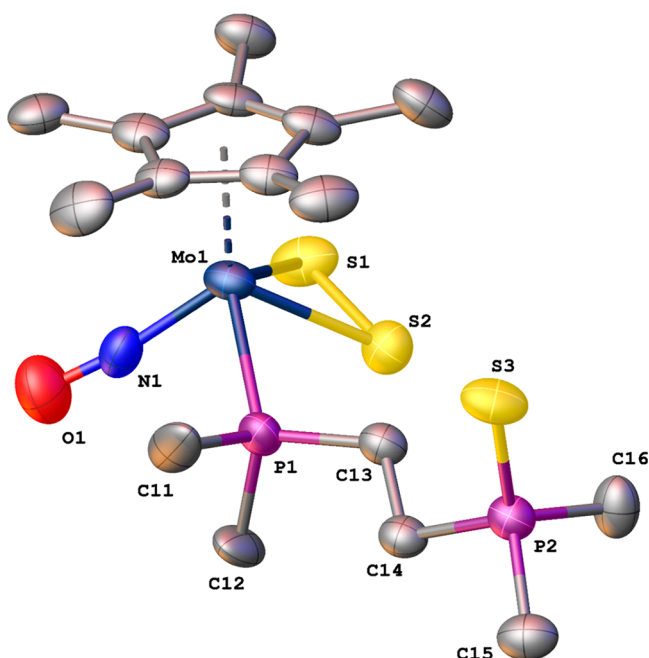


Figure 4. Solid-state molecular structure of $\text{Cp}^*\text{Mo}(\text{NO})(\eta^2\text{-S}_2)(\kappa^1\text{-dmpeS})$ (**4**) with 50% probability thermal ellipsoids shown. Hydrogen atoms were omitted for the sake of clarity. Selected bond lengths (Å) and angles (deg): Mo(1)–S(1) = 2.450(5), Mo(1)–S(2) = 2.459(4), Mo(1)–P(1) = 2.4696(13), Mo(1)–N(1) = 1.825(5), N(1)–O(1) = 1.172(6), S(1)–S(2) = 2.059(4), P(1)–C(11) = 1.843(8), P(1)–C(12) = 1.797(7), P(1)–C(13) = 1.834(5), C(13)–C(14) = 1.523(7), P(2)–S(3) = 1.962(2), P(2)–C(14) = 1.807(5), P(2)–C(15) = 1.817(6), P(2)–C(16) = 1.792(5), Mo(1)–N(1)–O(1) = 170.1(5), S(1)–Mo(1)–S(2) = 49.61(9), S(2)–Mo(1)–P(1) = 76.00(8), P(1)–Mo(1)–N(1) = 82.20(14), N(1)–Mo(1)–S(1) = 95.55(19), S(1)–S(2)–Mo(1) = 64.98(16), S(2)–S(1)–Mo(1) = 65.41(18).

which is similar to that extant in **3** and an essentially linear Mo(1)–N(1)–O(1) linkage of 170.1(5)°.

Because treatment of **3** with additional sulfur also results in the production of **4**, it is likely that the oxidation of **2** by elemental sulfur proceeds in a stepwise manner. In the first step, the sulfur effects the oxidation of one end of the dmpe ligand to transiently form $[\text{Cp}^*\text{Mo}(\text{NO})(\kappa^2\text{-dmpeS})]$, which contains the hemilabile dmpeS ligand.¹⁶ Dissociation of the sulfur donor site from the molybdenum's coordination sphere then generates the 16e $[\text{Cp}^*\text{Mo}(\text{NO})(\kappa^1\text{-dmpeS})]$ fragment. Interestingly, this fragment does not activate the benzene solvent to form 18e $\text{Cp}^*\text{Mo}(\text{NO})(\kappa^1\text{-dmpeS})(\text{H})(\text{Ph})$ but

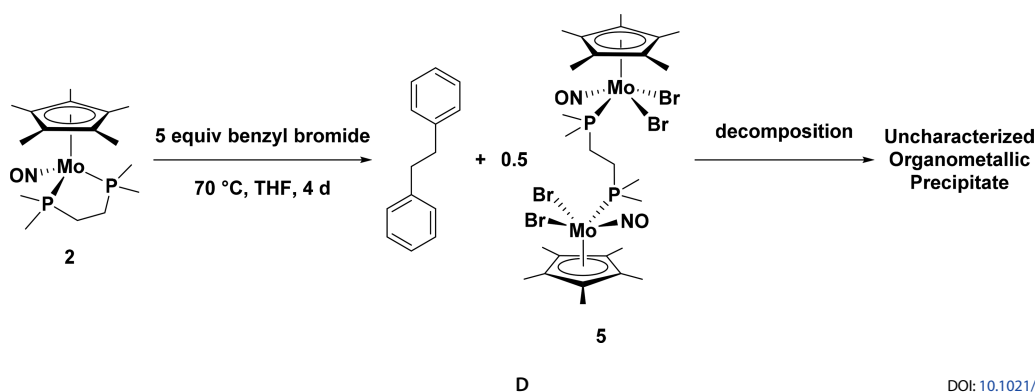
rather incorporates another sulfur atom on the way to forming the Mo=S=Mo bridge in $(\mu\text{-S})[\text{Cp}^*\text{Mo}(\text{NO})(\kappa^1\text{-dmpeS})]_2$ (**3**). The last step to form $\text{Cp}^*\text{Mo}(\text{NO})(\eta^2\text{-S}_2)(\kappa^1\text{-dmpeS})$ (**4**) involves cleavage of the Mo=S=Mo bridge by additional sulfur atoms with concomitant formation of the $\eta^2\text{-S}_2$ ligand at each molybdenum so that the favored 18e configuration can be maintained.

Reaction of $\text{Cp}^*\text{Mo}(\text{NO})(\kappa^2\text{-dmpe})$ with an Excess of O_2 . Exposure of an Et_2O solution of **2** to an oxygen atmosphere results in the formation of a yellow precipitate which has only been partially characterized because all attempts to purify it by chromatography or crystallization have been unsuccessful to date. Nevertheless, NMR and MS data are consistent with the yellow solid being formed by the uptake of either 1 or 2 equiv of oxygen by the initial reactant. For example, the $^{31}\text{P}\{^1\text{H}\}$ NMR spectrum of the yellow solid in C_6D_6 (Figure S17) exhibits two doublets at chemical shifts comparable to those in the analogous spectra of **3** and **4**, thereby indicating the formation of an organometallic complex in which the two phosphorus atoms in the possibly modified dmpe ligand are no longer chemically equivalent.

Reaction of $\text{Cp}^*\text{Mo}(\text{NO})(\kappa^2\text{-dmpe})$ with Benzyl Bromide. Oxidation of **2** with 5 equiv of benzyl bromide in THF results in the formation of the bimetallic Mo(II) complex $(\mu\text{-dmpe})[\text{Cp}^*\text{Mo}(\text{NO})\text{Br}_2]_2$ (**5**) and bibenzyl after 4 d at 70 °C (Scheme 5). During the course of the reaction, the initial orange solution darkens and deposits a molybdenum-containing beige precipitate whose identity remains unknown. The bibenzyl product can be isolated in 71% yield by flash silica column chromatography with hexanes as the eluant. A small amount of X-ray quality orange crystals of **5** was obtained on only one occasion by slow cooling of the reaction mixture, but other attempts to purify **5** from the THF supernatant solution by column chromatography or crystallization were unsuccessful to date. For instance, addition of pentane to the THF supernatant solution results in the immediate deposition of the beige precipitate that is initially formed during the reaction. It thus appears that **5** is a thermally unstable intermediate complex that does not persist in solution but slowly converts to the as yet uncharacterized organometallic precipitate.

The formation of bibenzyl suggests that a possible mechanism for the reaction shown in Scheme 5 involves radical species. Many examples of reactions involving the homolytic cleavage of alkyl–halide bonds and atom-transfer processes resulting in the formation of alkyl radicals and metal–halides are described in the literature.^{17–22} For instance, the anionic pincer complex, $[\text{PCP}\text{-Pt}^0]^-$ [$\text{PCP} = \text{C}_6\text{H}_3(\text{CH}_2\text{Pt-Bu}_2)_2$], reacts with benzyl chloride in THF and forms PCP-

Scheme 5. Reaction of $\text{Cp}^*\text{Mo}(\text{NO})(\kappa^2\text{-dmpe})$ with Benzyl Bromide



PtCl and bibenzyl.²³ Nevertheless, the detailed mechanism for the conversion shown in Scheme 5 remains to be ascertained.

The solid-state molecular structure of **5** is shown in Figure 5. The two halves of the bimetallic complex are related by a center

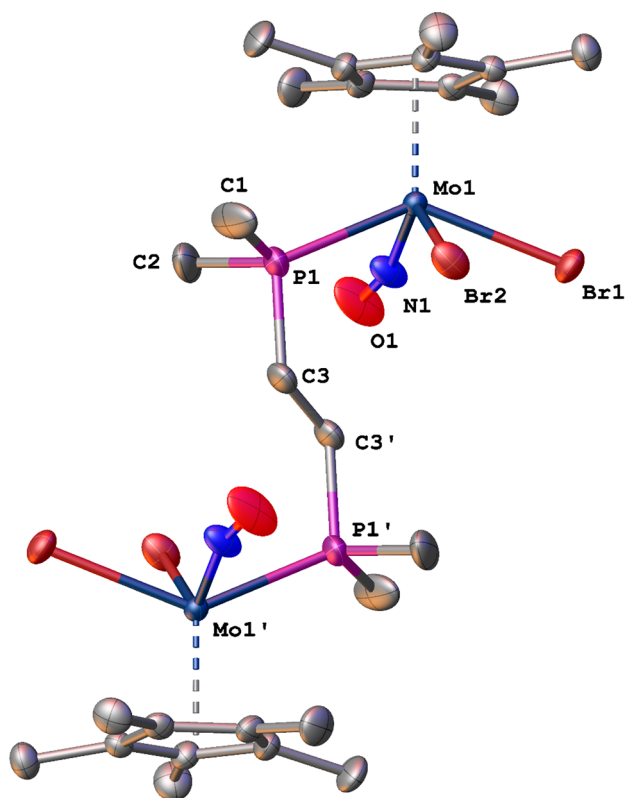


Figure 5. Major disordered fragment of the solid-state molecular structure of **5** with 50% probability thermal ellipsoids shown. Hydrogen atoms were omitted, and only one-half of the molecule was fully labeled for the sake of clarity. Selected bond lengths (Å) and angles (deg): Mo(1)–Br(1) = 2.6068(6), Mo(1)–Br(2) = 2.6014(8), Mo(1)–P(1) = 2.492(7), Mo(1)–N(1) = 1.806(8), N(1)–O(1) = 1.144(9), P(1)–C(1) = 1.810(9), P(1)–C(2) = 1.841(8), P(1)–C(3) = 1.837(7), C(3)–C(3') = 1.532(15), Br(1)–Mo(1)–Br(2) = 80.79(3), Br(2)–Mo(1)–P(1) = 74.39(18), P(1)–Mo(1)–N(1) = 82.8(3), N(1)–Mo(1)–Br(1) = 82.08(19), Mo(1)–N(1)–O(1) = 165.5(7).

of inversion, and both molybdenum centers are in four-legged piano-stool geometries capped by Cp* rings. A single dmpe ligand forms the bridge between the two metal centers. The nitrosyl ligands are essentially linear with Mo–N–O bond angles of 165.5(7)°, and the Mo–P bond lengths of 2.492(7) Å are comparable to those found in related complexes (vide supra).

Reaction of Cp*Mo(NO)(κ²-dmpe) with 1-Bromopropane. A THF solution of **2** containing 5 equiv of 1-bromopropane results in the deposition of a red crystalline

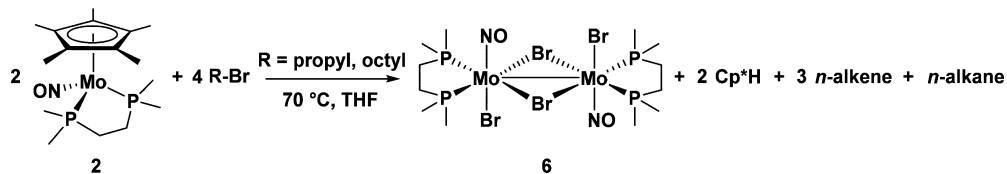
precipitate and the formation of a pale yellow supernatant solution after 72 h at 70 °C. The crystalline product can be isolated in 69% yield by decanting away the supernatant solution and washing the crystals with THF. The crystals are of sufficient quality for a single-crystal X-ray diffraction analysis that has revealed them to be the Mo(II) complex [Mo(NO)-Br₂(κ²-dmpe)]₂ (**6**). The oxidation reaction shown in Scheme 6 involves the loss of the Cp* ligand and the incorporation of two bromine atoms per metal center from the 1-bromopropane reactant. A molybdenum–molybdenum single bond is invoked in **6** to allow both metal centers to attain the favored 18e configuration

All spectroscopic evidence is consistent with **6** having the structure depicted in Scheme 6. The bimetallic complex exhibits a ν(NO) band in its IR spectrum at 1619 cm⁻¹ with a shoulder at 1577 cm⁻¹ attributable to the asymmetric stretch of the nitrosyl ligands. The complex is completely insoluble in most NMR solvents and is only sparingly soluble in CD₂Cl₂. The ¹H, ¹³C{¹H}, and ³¹P{¹H} NMR spectra of **6** in CD₂Cl₂ are as expected and indicate that the nuclei in the two κ²-dmpe ligands are in chemically equivalent environments. The ¹H NMR spectrum (Figure S18) consists of four resonances attributable to the two groups of methyl protons and the two groups of methylene protons that are either proximal or distal to the nitrosyl ligands. Consistently, the ³¹P{¹H} NMR spectrum (Figure S20) displays a lone singlet at δ 35.4 ppm.

¹H NMR spectroscopic and GCMS analyses of the supernatant solution indicate that the organic portions of the reactants in the reaction involving 1-bromopropane are converted into Cp*H, propene, and propane. Regrettably, the amounts of propane and propene cannot be quantified by GCMS because they coelute from the GC column and overlap in the chromatogram. Furthermore, due to both the volatility of propane and propene as well as the presence of unreacted 1-bromopropane that dominates certain regions in the ¹H NMR spectrum of the final reaction mixture, NMR analysis is also unable to quantify the relative amounts of the organic products.

A notable feature of the transformation depicted in Scheme 6 is the loss of the Cp* ligand from **2**. The Cp* ligand is ubiquitous in transition-metal organometallic chemistry, and when coordinated to a transition-metal center, it often remains as a spectator ligand. On rare occasions it can be a participant in the chemistry exhibited by its molecular scaffolds while remaining coordinated to the metal center. For instance, under a variety of experimental conditions, the C–H bond activation of a methyl group in coordinated Cp* ligands was shown to result in the formation of either η²:η⁴ or η¹:η⁵ tetramethylfulvene-like ligands via H atom abstraction.²⁴ Recently, it has also been reported that treatment of 18e Cp*Rh(bpy) [bpy = κ²-2,2'-bipyridine] with a protonic acid initially affords the 16e pentamethylcyclopentadiene-containing cation, [(η⁴-Cp*H)Rh(bpy)]⁺, which is believed to result from the C–H bond-forming reductive elimination from the transient rhodium hydrido complex, [Cp*Rh(bpy)H]⁺.^{25,26}

Scheme 6. Balanced Reactions of Cp*Mo(NO)(κ²-dmpe) with 1-Bromopropane and 1-Bromooctane



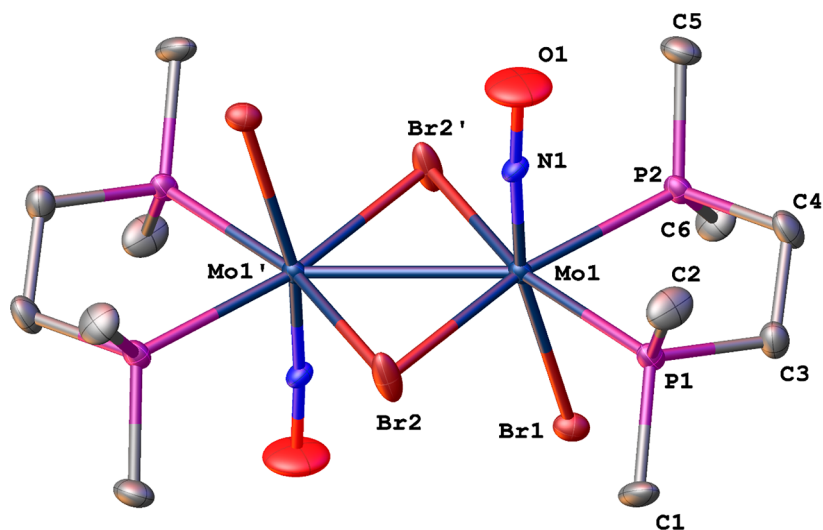


Figure 6. Major component of the solid-state molecular structure of **6** with 50% probability thermal ellipsoids shown. Hydrogen atoms were omitted, and only one-half of the molecule was fully labeled for the sake of clarity. Selected bond lengths (Å) and angles (deg): Mo(1)–Mo(1)' = 2.9819(10), Mo(1)–Br(1) = 2.6315(19), Mo(1)–Br(2) = 2.5847(9), Mo(1)–Br(2)' = 2.5871(9), Mo(1)–P(1) = 2.4790(17), Mo(1)–P(2) = 2.4825(17), Mo(1)–N(1) = 1.776(13), N(1)–O(1) = 1.35(2), P(1)–C(1) = 1.811(7), P(1)–C(2) = 1.801(7), P(1)–C(3) = 1.824(7), P(2)–C(4) = 1.834(7), P(2)–C(5) = 1.804(7), P(2)–C(6) = 1.821(7), C(3)–C(4) = 1.525(10), Mo(1)–N(1)–O(1) = 175.2(13), Mo(1)–Br(2)–Mo(1)' = 70.42(3), Mo(1)'–Mo(1)–N(1) = 94.0(3), Mo(1)'–Mo(1)–Br(1) = 98.64(4), P(1)–Mo(1)–P(2) = 80.53(6), Br(2)–Mo(1)–Br(2)' = 109.58(3), P(1)–Mo(1)–Br(2) = 85.58(4), P(2)–Mo(1)–Br(2)' = 84.35(4).

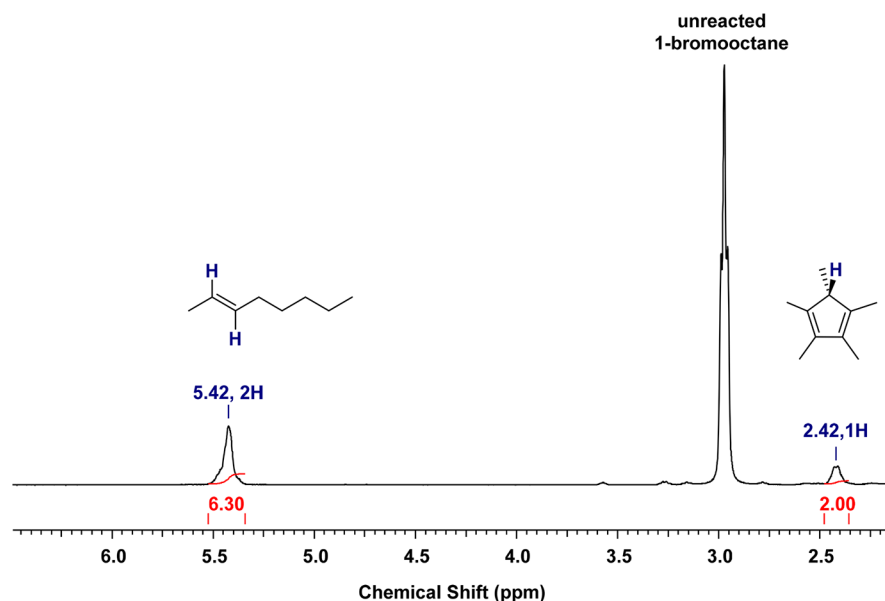


Figure 7. Expansion of the ^1H NMR spectrum (400 MHz, C_6D_6) from δ 2.14 to 6.44 ppm showing the resonances attributable to the two methine protons of *trans*-2-octene and the single nonmethyl proton of pentamethylcyclopentadiene and their relative integrations.

Even rarer are the cases in which Cp^*H is liberated as the free diene, having been previously reported for the solvent-induced elimination of Cp^*H from $[\text{Cp}^*\text{Ir}(\text{H})_3(\text{PPh}_3)]^{+27}$ and the phosphine-induced liberation from $\text{Cp}^*\text{Rh}(\text{H})_2(\text{PMe}_3)$.²⁸ During the conversion shown in Scheme 6, the Cp^* ligand is not only a participant in the characteristic reactivity of **2** but is subsequently liberated from the transition metal's coordination sphere as free Cp^*H . This aspect is unique for $\text{Cp}^*\text{Mo}(\text{NO})-(\kappa^2\text{-dmpe})$ (**2**) because, during the chemistry exhibited by other $\text{Cp}^*\text{M}(\text{NO})$ -containing complexes ($\text{M} = \text{Mo}$ or W), the 14e fragment remains intact throughout all the chemical transformations.¹ The exact mechanism of the reaction of **2** with bromoalkanes such as 1-bromopropane that results in the

liberation of Cp^*H (i.e., whether it involves the reductive elimination of a hydrido and the Cp^* ligand from the transition metal's coordination sphere or radical processes wherein hydrogen radicals couple with the Cp^* rings, or some other mechanism entirely) remains to be ascertained.

The solid-state molecular structure of complex **6** was established by a single-crystal X-ray diffraction analysis, and it is shown in Figure 6. The structure is that of a bimetallic complex in which the two halves of the molecule are related by an inversion center, and the two molybdenum centers are in a pseudo-octahedral coordination geometry. Two bromine atoms form bridging linkages between the molybdenum centers with Mo–Br bond lengths that are essentially the same. A metal–

metal single bond exists in the structure with the Mo–Mo bond length of 2.9819(10) Å, being comparable to other such linkages described in the literature.^{12,29,30} Finally, the nitrosyl ligand is part of a disordered system and shares space with the much larger Br atom, a fact that results in a distortion of the N–O bond length.

Reaction of Cp*Mo(NO)(κ²-dmpe) with 1-Bromooctane. 1-Bromooctane was used as the alkyl halide reactant instead of 1-bromopropane to produce less volatile organic products that are easier to quantify as compared to those resulting from the reaction with 1-bromopropane. As expected, reaction of 5 equiv of 1-bromooctane with **2** in a THF solution at 70 °C affords a pale yellow supernatant solution and red crystals of [Mo(NO)Br₂(κ²-dmpe)]₂ (**6**) after 16 h (Scheme 6). GCMS and ¹H NMR analyses of the supernatant solution indicate the principal organic products of the reaction to be Cp*H, octane and *trans*-2-octene with trace amounts of 1-octene and *cis*-2-octene. The ¹H NMR spectrum of the supernatant solution (Figure 7) also shows that *trans*-2-octene and Cp*H are present in a 3:2 ratio, respectively. As depicted in Scheme 6, the experimental data thus indicates that the reaction involves two equiv of **2** and four equiv of 1-bromooctane being transformed into one equiv of the dimeric complex **6** accompanied by three equiv of *trans*-2-octene and 1 equiv of octane. The mechanism of this remarkable conversion remains to be established.

Reaction of Cp*Mo(NO)(κ²-dmpe) with 1,5-Dibromopentane. Given the chemistry exhibited by complex **2** with monobrominated alkanes, investigations into its reactions with terminal dibromoalkanes were initiated. Treatment of Cp*Mo(NO)(κ²-dmpe) with an excess of 1,5-dibromopentane under the same experimental conditions as previous reactions gives the expected outcome, namely the loss of the Cp* ligand as Cp*H, formation of the dimeric complex **6**, 1-bromopentane, and a bromoalkene. It appears that when a large excess of 1,5-dibromopentane is employed, one brominated terminus of the starting alkane does not undergo any reactivity, and therefore the reaction proceeds in the same manner as the monobrominated alkanes (Scheme 6). The exact identity of the alkene formed is not known with certainty because its analyses by GCMS and NMR spectroscopy have not given consistent results.

In an attempt to induce cyclization of 1,5-dibromopentane, its reaction with **2** was repeated but with a stoichiometric amount of the dibromoalkane. Unfortunately, the reaction is not straightforward, and multiple reaction pathways appear to be occurring. Thus, in addition to the pathway resulting in loss of Cp*H and formation of **6** and its associated organic products (cf. Scheme 6), the reaction pathway described in the reaction of **2** with benzyl bromide (Scheme 5) also occurs, and decomposition products are formed. In addition, GCMS and ¹H NMR data suggest the presence of 2-pentene and cyclopentene in the final reaction mixture.

Attempted Reactions of Cp*Mo(NO)(κ²-dmpe) with Other Hydrocarbyl Halides. Interestingly, complex **2** does not display any reactivity with bromobenzene or 1-bromoadamantane even after heating for several days at 70 °C. Similar experiments of **2** with 1-chloroalkanes also produce no detectable changes, whereas 1-iodoalkanes under similar reaction conditions produce intractable mixtures of products.

CONCLUSION

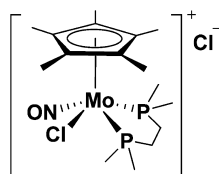
This study demonstrated that hemilability of the symmetrically bound dmpe ligand in Cp*Mo(NO)(κ²-dmpe) (**2**) can be induced by exposing the electron-rich complex to oxidizing conditions. Thus, reactions of a benzene solution of **2** with either an equimolar amount or an excess of elemental sulfur afford (μ-S)[Cp*Mo(NO)(κ¹-dmpeS)]₂ (**3**) and Cp*Mo(NO)(η²-S₂)(κ¹-dmpeS) (**4**), respectively. In both **3** and **4**, one phosphorus end of the dmpe ligand in **2** was displaced from the molybdenum's coordination sphere and converted into a phosphine sulfide linkage. In a related reaction, exposure of **2** to 5 equiv benzyl bromide in THF produces the bimetallic complex (μ-dmpe)[Cp*Mo(NO)Br₂]₂ (**5**), in which the dmpe ligand links the two metal centers. In contrast, complex **2** forms [Mo(NO)Br₂(κ²-dmpe)]₂ (**6**), olefin, alkane, and Cp*H when treated with 5 equiv of 1-bromopropane, 1-bromooctane, or 1,5-dibromopentane in THF at 70 °C. The mechanisms of these latter transformations as well as other aspects of the characteristic chemical properties of Cp*Mo(NO)(κ²-dmpe) remain to be investigated.

EXPERIMENTAL SECTION

General Methods. All reactions and subsequent manipulations involving organometallic reagents were performed under anhydrous and anaerobic conditions except where noted. High-vacuum and inert-atmosphere techniques were performed using double-manifold Schlenk lines or in Innovative Technologies LabMaster 100 and MS-130 BG dual-station gloveboxes equipped with freezers maintained at –30 °C. Preparative scale reactions were performed with Schlenk or round-bottom flasks; reactions were performed in thick-walled glass reaction flasks (larger scale) or J. Young NMR tubes (smaller scale), both of which were typically sealed with Kontes greaseless stopcocks. Tetrahydrofuran (THF) and diethyl ether (Et₂O) were dried over sodium/benzophenone ketyl and freshly distilled prior to use; *n*-pentane was dried over calcium hydride and freshly distilled prior to use; all other solvents were dried according to standard procedures.³¹ Cp*Mo(NO)Cl₂ was prepared according to the published procedure.⁵ Pentamethylcyclopentadiene was obtained from the Boulder Scientific Co. All other chemicals and reagents were ordered from commercial suppliers and used as received.

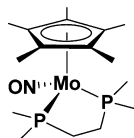
Unless otherwise specified, all IR samples were prepared as Nujol mulls sandwiched between NaCl plates, and their spectra were recorded on a Thermo Nicolet model 4700 FT-IR spectrometer. Except where noted, all NMR spectra were recorded at room temperature on a Bruker AV-400 instrument (direct and indirect probes), and all chemical shifts are reported in ppm and coupling constants in Hz. ¹H NMR spectra were referenced to the residual protio isotopomer present in C₆D₆ (7.16 ppm) or CD₂Cl₂ (5.32 ppm). ¹³C NMR spectra were referenced to C₆D₆ (128.39 ppm) or CD₂Cl₂ (53.84 ppm). ³¹P NMR spectra were externally referenced to 85% H₃PO₄. For the characterization of most complexes, two-dimensional NMR experiments, {¹H–¹H} COSY, {¹H–¹³C} HSQC, {¹H–³¹P} HMBBC, and {¹H–¹³C} HMBBC were performed to correlate and assign ¹H, ¹³C, and ³¹P NMR signals and establish atom connectivity. GC analyses were performed on an Agilent Technologies 7890B GC equipped with a HP-SMS (30 m × 0.250 mm × 0.25 μm) capillary column coupled to an Agilent Technologies 5977A MSD analyzer. Low- and high-resolution mass spectra (EI, 70 eV) and MALDI-TOF spectra were recorded by M. Lapawa of the UBC mass spectrometry facility using a Kratos MS-50 spectrometer and a Bruker Autoflex spectrometer, respectively. M. Yung recorded ESI mass spectra on a Bruker HCT spectrometer. Elemental analyses were performed by D. Smith, and GC analyses were performed by Dr. Y. Ling and M. Lapawa in the UBC microanalytical facility. X-ray crystallographic data collection, solution, and refinement were performed at the UBC X-ray crystallography facility.

Preparation of $[\text{Cp}^*\text{Mo}(\text{NO})(\kappa^2\text{-dmpe})\text{Cl}]\text{Cl}$ (1). In a glovebox, a Schlenk flask was loaded with $\text{Cp}^*\text{Mo}(\text{NO})\text{Cl}_2$ (0.200 g, 0.602 mmol) and a stir bar. Also in the glovebox, another Schlenk flask was charged with dmpe (0.10 mL, 0.60 mmol). On a double manifold, THF (ca. 50 mL) was cannulated into both flasks, affording a bright green solution and a colorless solution, respectively. The dmpe solution was then transferred by cannula into the flask containing the stirred $\text{Cp}^*\text{Mo}(\text{NO})\text{Cl}_2$ solution, whereupon the color of the reaction mixture changed from green to yellow, and a yellow precipitate formed. After 10 min, the solvent was decanted, and the remaining solid was washed with THF (2 \times 20 mL) before being taken to dryness in vacuo to obtain $[\text{Cp}^*\text{Mo}(\text{NO})(\text{Cl})(\kappa^2\text{-dmpe})]\text{Cl}$ (1) as a fine yellow powder (0.189 g, 0.392 mmol, 65% yield). Recrystallization of 1 from 1:1 CH_2Cl_2 /hexanes in an aerobic environment afforded small yellow crystals of $[\text{Cp}^*\text{Mo}(\text{NO})(\text{Cl})(\kappa^2\text{-dmpe})]\text{Cl}\cdot 2\text{H}_2\text{O}$ that were subjected to an X-ray diffraction analysis.



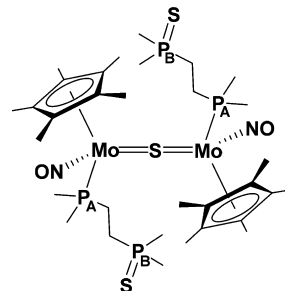
Characterization data for $[\text{Cp}^*\text{Mo}(\text{NO})(\text{Cl})(\kappa^2\text{-dmpe})]\text{Cl}$ (1): IR (cm^{-1}): 1661 (s, ν_{NO}). MALDI-TOF (dtcb/ CDCl_3 , m/z): 448.2 for $\text{C}_{16}\text{H}_{31}\text{ClNOP}_2\text{Mo}$ ($[\text{M} - \text{Cl}]^+$, ^{98}Mo). HRMS-ESI(+) (40 V, m/z): ($[\text{M} - \text{Cl}]^+$, ^{92}Mo) calcd for $\text{C}_{16}\text{H}_{31}\text{ClNOP}_2^{92}\text{Mo}$, 442.0638; found, 442.0633. ^1H NMR (400 MHz, CD_2Cl_2): δ 1.75 (d, $^2J_{\text{HP}} = 10.4$, 3H, PMe), 1.81 (d, $^2J_{\text{HP}} = 10.8$, 3H, PMe), 1.84 (d, $^2J_{\text{HP}} = 10.6$, 3H, PMe), 2.00 (s, 15H, C_5Me_5), 2.03–2.11 (overlapped m, 1H, $\text{PCH}_2\text{CH}_2\text{P}$), 2.19 (d, $^2J_{\text{HP}} = 10.0$, 3H, PMe), 2.40–2.49 (m, 1H, $\text{PCH}_2\text{CH}_2\text{P}$), 2.81–2.94 (overlapped m, 2H, $\text{PCH}_2\text{CH}_2\text{P}$). ^{13}C APT NMR (100 MHz, CD_2Cl_2): δ 10.6 (d, $^1J_{\text{CP}} = 28.8$, PMe), 11.4 (C_5Me_5), 12.9 (d, $^1J_{\text{CP}} = 28.0$, PMe), 15.4 (d, $^1J_{\text{CP}} = 21.5$, PMe), 17.6 (d, $^1J_{\text{CP}} = 36.8$, PMe), 25.4 (dd, $^1J_{\text{CP}} = 27.6$, $^2J_{\text{CP}} = 8.4$, $\text{PCH}_2\text{CH}_2\text{P}$), 33.7 (dd, $^1J_{\text{CP}} = 36.4$, $^2J_{\text{CP}} = 14.6$, $\text{PCH}_2\text{CH}_2\text{P}$), 117.2 (C_5Me_5). $^{31}\text{P}\{^1\text{H}\}$ NMR (162 MHz, CD_2Cl_2): δ 37.4 (d, $^2J_{\text{PP}} = 45.6$, MoP), 44.9 (d, $^2J_{\text{PP}} = 45.6$, MoP). Anal. Calcd for $\text{C}_{16}\text{H}_{31}\text{Cl}_2\text{NOP}_2\text{Mo}$: C, 39.85; H, 6.48; N, 2.90. Found: C, 39.77; H, 6.58; N, 2.62.

Preparation of $\text{Cp}^*\text{Mo}(\text{NO})(\kappa^2\text{-dmpe})$ (2). In a glovebox, a Schlenk flask was charged with $\text{Cp}^*\text{Mo}(\text{NO})\text{Cl}_2$ (1.002 g, 3.017 mmol) and a stir bar, a second Schlenk flask with dmpe (0.51 mL, 3.0 mmol), and a third Schlenk flask with Cp_2Co (1.142 g, 6.038 mmol). The $\text{Cp}^*\text{Mo}(\text{NO})\text{Cl}_2$ and dmpe were reacted in the manner described in the preceding section to obtain $[\text{Cp}^*\text{Mo}(\text{NO})(\text{Cl})(\text{dmpe})]\text{Cl}$ (1) as a yellow powder. CH_2Cl_2 (ca. 100 mL) was then cannulated into the flask to obtain a clear yellow solution. The Cp_2Co was dissolved in CH_2Cl_2 (ca. 30 mL), and this solution was then added dropwise to the yellow solution, whereupon it became black. The reaction mixture was stirred for 30 min to obtain a clear, dark red supernatant solution that was removed by filter cannulation. Removal of the solvent from the filtered solution in vacuo and recrystallization of the residue from Et_2O afforded $\text{Cp}^*\text{Mo}(\text{NO})(\kappa^2\text{-dmpe})$ (2) as dark red crystals (0.449 g, 1.092 mmol, 36% yield).



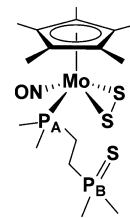
Characterization data for $\text{Cp}^*\text{Mo}(\text{NO})(\kappa^2\text{-dmpe})$ (2). IR (cm^{-1}): 1535 (s, ν_{NO}). MS (LREI m/z , probe temperature 150 $^\circ\text{C}$) 413 [M^+ , ^{98}Mo]. MS (HREI, m/z , ^{92}Mo): calcd 407.09449, found 407.09490. ^1H NMR (400 MHz, C_6D_6): δ 0.92 (d, $^2J_{\text{HP}} = 6.5$, 6H, PMe), 1.07 (m, 2H, CH), 1.29 (m, 2H, CH), 1.39 (d, $^2J_{\text{HP}} = 8.4$, 6H, PMe), 1.95 (s, 15H, C_5Me_5). ^{13}C APT NMR (100 MHz, C_6D_6): δ 12.2 (C_5Me_5), 16.7 (m, PMe), 19.2 (m, PMe), 31.9 (m, PCH_2), 101.2 (C_5Me_5). $^{31}\text{P}\{^1\text{H}\}$ NMR (162 MHz, C_6D_6): δ 57.1 (s, MoP). Anal. Calcd for $\text{C}_{16}\text{H}_{31}\text{MoNOP}_2$: C, 46.72; H, 7.60; N, 3.41. Found: C, 46.80; H, 7.37; N, 3.19.

Preparation of $(\mu\text{-S})[\text{Cp}^*\text{Mo}(\text{NO})(\kappa^1\text{-dmpeS})]_2$ (3). In a glovebox, a thick-walled flask was charged with $\text{Cp}^*\text{Mo}(\text{NO})(\kappa^2\text{-dmpe})$ (0.084 g, 0.205 mmol), C_6H_6 (ca. 20 mL), and a magnetic stir bar. On a double manifold, elemental sulfur (0.007 g, 0.218 mmol) was added to the vessel, whereupon the stirred orange solution immediately developed a brown coloration, and a precipitate formed. The solvent was removed in vacuo to obtain a blue powder that was purified by column chromatography over basic alumina (1 \times 4 cm) made up in Et_2O . Elution of the column with 1:1 THF: Et_2O developed a dark blue band that was eluted and collected. Removal of solvents from the eluate under reduced pressure afforded $(\mu\text{-S})[\text{Cp}^*\text{Mo}(\text{NO})(\kappa^1\text{-dmpeS})]_2$ (3) as a dark blue solid (0.032 g, 0.035 mmol, 48% yield). Recrystallization of 3 from a 1:10 pentane:benzene solution left at ambient temperatures for 15 d afforded small blue crystals of sufficient quality for a single-crystal X-ray diffraction analysis.



Characterization data for $(\mu\text{-S})[\text{Cp}^*\text{Mo}(\text{NO})(\kappa^1\text{-dmpeS})]_2$ (3): IR (cm^{-1}): 1562 (s, ν_{NO}). ESI(+)-MS (40 V); m/z 445.1 for $\text{C}_{16}\text{H}_{31}\text{NOP}_2\text{SMo}$ (M^+ , ^{98}Mo). HRMS-ESI(+) (40 V, m/z): ($[\text{M} + \text{H}]^+$, ^{92}Mo) calcd for $\text{C}_{16}\text{H}_{32}\text{NOP}_2\text{S}^{92}\text{Mo}$, 440.0748; found, 440.0748. ^1H NMR (400 MHz, C_6D_6): δ 1.07 (d, $^2J_{\text{HP}} = 7.9$, 3H, P_AMe), 1.36 (d, $^2J_{\text{HP}} = 12.9$, 3H, P_BMe), 1.37 (d, $^2J_{\text{HP}} = 8.1$, 3H, P_AMe), 1.39 (d, $^2J_{\text{HP}} = 12.8$, 3H, P_BMe), 1.87 (s, 15H, C_5Me_5), 1.88 (overlapped m, 1H, P_ACH_2), 2.02 (m, 1H, P_BCH_2), 2.19 (m, 1H, P_ACH_2), 2.37 (m, 1H, P_BCH_2). ^{13}C APT NMR (100 MHz, C_6D_6): δ 11.6 (C_5Me_5), 14.4 (d, $^1J_{\text{CP}} = 27.9$, P_AMe), 15.8 (d, $^1J_{\text{CP}} = 23.9$, P_AMe), 20.4 (d, $^1J_{\text{CP}} = 53.3$, P_BMe), 21.6 (d, $^1J_{\text{CP}} = 55.5$, P_BMe), 25.4 (d, $^1J_{\text{CP}} = 26.0$, P_ACH_2), 30.0 (d, $^1J_{\text{CP}} = 51.5$, P_BCH_2), 107.9 (C_5Me_5). $^{31}\text{P}\{^1\text{H}\}$ NMR (162 MHz, C_6D_6): δ 22.7 (d, $^3J_{\text{PP}} = 47.6$, MoP_A), 39.2 (d, $^3J_{\text{PP}} = 47.6$, SP_B).

Preparation of $\text{Cp}^*\text{Mo}(\text{NO})(\eta^2\text{-S}_2)(\kappa^1\text{-dmpeS})$ (4). In a glovebox, a thick-walled flask was charged with $\text{Cp}^*\text{Mo}(\text{NO})(\kappa^2\text{-dmpe})$ (0.164 g, 0.400 mmol), C_6H_6 (ca. 30 mL), and a magnetic stir bar to obtain a bright orange solution. To this solution was added an excess of elemental sulfur (0.064 g, 2.00 mmol) on a double manifold whereupon the reaction mixture became a dark red-brown in color. The solvent was removed in vacuo, and the remaining brown residue was purified by column chromatography on a basic alumina column (1 \times 4 cm) made up in Et_2O . Elution of the column with 1:1 THF: Et_2O developed a single red band that was eluted and collected. Removal of solvents from the eluate under reduced pressure afforded $\text{Cp}^*\text{Mo}(\text{NO})(\eta^2\text{-S}_2)(\kappa^1\text{-dmpeS})$ (4) as a red solid (0.083 g, 0.163 mmol, 41% yield). Small red crystals of 4 suitable for an X-ray diffraction analysis were obtained by vapor diffusion of Et_2O into a C_6H_6 solution of the complex over 3 d at ambient temperatures.



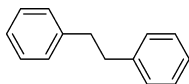
Characterization data for $\text{Cp}^*\text{Mo}(\text{NO})(\eta^2\text{-S}_2)(\kappa^1\text{-dmpeS})$ (4): IR (cm^{-1}): 1593 (s, ν_{NO}). MS (LREI, m/z , probe temperature 150 $^\circ\text{C}$): 509 [M^+ , ^{98}Mo], 445 [$\text{M}^+ - \text{S}_2$, ^{98}Mo]. MS (HREI, m/z , ^{92}Mo): calcd 503.01112, found 503.01123. ^1H NMR (400 MHz, C_6D_6): δ 1.03 (d, $^2J_{\text{HP}} = 8.8$, 3H, P_AMe), 1.07 (d, $^2J_{\text{HP}} = 8.8$, 3H, P_AMe), 1.12 (d, $^2J_{\text{HP}} = 12.7$, 3H, P_BMe), 1.17 (d, $^2J_{\text{HP}} = 12.7$, 3H, P_BMe), 1.62 (s, 15H,

C_5Me_5), 1.71 (m, 1H, P_BCH_2), 1.82 (m, 1H, P_BCH_2), 2.27 (m, 1H, P_ACH_2), 2.35 (m, 1H, P_ACH_2). ^{13}C APT NMR (100 MHz, C_6D_6): δ 10.7 (C_5Me_5), 12.5 (d, $^1J_{CP} = 26.0$, P_AMe), 13.4 (d, $^1J_{CP} = 28.7$, P_AMe), 20.4 (d, $^1J_{CP} = 54.0$, P_BMe), 21.2 (d, $^1J_{CP} = 54.9$, P_BMe), 28.5 (dd, $^1J_{CP} = 35.6$, $^2J_{CP} = 3.0$, P_ACH_2), 29.5 (dd, $^1J_{CP} = 50.8$, $^2J_{CP} = 0.9$, P_BCH_2), 110.8 (C_5Me_5). $^{31}P\{^1H\}$ NMR (162 MHz, C_6D_6): δ 21.8 (d, $^3J_{PP} = 48.5$, MoP_A), 37.9 (d, $^3J_{PP} = 49.5$, SP_B).

Reaction of $Cp^*Mo(NO)(\kappa^2-dmpe)$ (2) with Excess O_2 . In a glovebox, a thick-walled flask was charged with $Cp^*Mo(NO)(\kappa^2-dmpe)$ (0.191 g, 0.464 mmol), Et_2O (ca. 20 mL), and a magnetic stir bar to form a bright orange solution. Immediately upon the introduction of 15 psig of O_2 into this flask outside the glovebox, the solution became brown and a yellow precipitate deposited. The solvent was removed from the final mixture under reduced pressure, and the remaining solid was washed with Et_2O (6×10 mL) before being taken to dryness in vacuo to obtain 0.123 g of a yellow solid. Further purification of this solid by column chromatography or recrystallization from mixtures of Et_2O , *n*-pentane, THF, and C_6H_6 has not been successful to date.

Partial characterization data for the yellow solid: ESI(+)-MS (40 V, m/z): 445.1 for $C_{16}H_{31}MoNO_3P_2$ ($[Cp^*Mo(NO)(dmpe) + O_2]^{+}$, ^{98}Mo), 429.2 for $C_{16}H_{31}MoNO_2P_2$ ($[Cp^*Mo(NO)(dmpe) + O]^{+}$, ^{98}Mo). 1H NMR (400 MHz, C_6D_6): δ 1.04 (d, $^2J_{HP} = 12.6$, 3H, PMe), 1.06 (d, $^2J_{HP} = 13.5$, 3H, PMe), 1.11 (d, $^2J_{HP} = 9.8$, 3H, PMe), 1.21 (d, $^2J_{HP} = 9.4$, 3H, PMe), 1.72 (s, 15H, C_5Me_5). $^{31}P\{^1H\}$ NMR (162 MHz, C_6D_6): δ 24.3 (d, $J_{PP} = 44.6$, MoP), 37.8 (d, $J_{PP} = 44.6$, MoP).

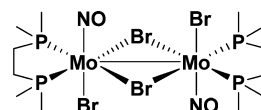
Reaction of $Cp^*Mo(NO)(\kappa^2-dmpe)$ (2) with Benzyl Bromide. In a glovebox, a flask was charged with 2 (0.076 g, 0.185 mmol) and THF (ca. 10 mL), resulting in a clear bright orange solution. On a double manifold, benzyl bromide (0.110 mL, 0.924 mmol) was added to the reaction flask via a micropipette. No immediate color change occurred. The flask and its contents were maintained at 70 °C for 4 d, after which time a beige precipitate had deposited, and the supernatant solution had become dark orange in color. Slow cooling of the supernatant solution to ambient temperatures resulted in the formation of red crystals on the sides of the flask. Analysis of these red crystals determined their identity to be $(\mu-dmpe)[Cp^*Mo(NO)(Br)_2]_2$ (5). Unfortunately, characterization of the complex was not possible because multiple attempts at repeating the reaction did not result in crystallization of the complex, and purification methods attempted on the supernatant solution resulted in the deposition of more of the beige precipitate that formed initially in the reaction vessel. The isolation of bibenzyl was carried out from a separate reaction wherein complex 2 (0.076 g, 0.185 mmol) and benzyl bromide (0.110 mL, 0.924 mmol) in THF were reacted in a manner identical to that described above. The supernatant solution was decanted into a separate flask, and the THF solvent was removed in vacuo. Column chromatography on flash silica of the remaining residue with hexanes as eluate afforded bibenzyl as a white crystalline solid (0.024 g, 0.132 mmol, 71% yield).



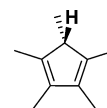
Partial characterization data for bibenzyl: MS (LREI, m/z , probe temperature 150 °C): 182 [M^+], 91 [$M^+ - CH_2Ph$]. 1H NMR (400 MHz, $CDCl_3$): δ 2.91 (s, 4H, CH_2), 7.17–7.29 (m, 10H, aryl H). These data match previously reported spectroscopic data.³²

Reaction of $Cp^*Mo(NO)(\kappa^2-dmpe)$ (2) with 1-Bromopropane. In a glovebox, a thick-walled flask was charged with complex 2 (0.101 g, 0.246 mmol) and THF (ca. 10 mL), resulting in a clear dark orange solution. On a double-manifold Schlenk line, 1-bromopropane (0.112 mL, 1.23 mmol) was added to the reaction flask using a micropipette. No color change occurred. The flask was heated to 70 °C, and the temperature was maintained for 4 d, after which time large dark red crystals had deposited from the now pale yellow solution. The supernatant solution was decanted from the flask, and the red crystals remaining were washed with THF (3×1 mL) before being dried in vacuo. $[Mo(NO)(Br)_2(dmpe)]_2$ (6) was collected as a red crystalline solid (0.074 g, 0.085 mmol, 69% yield). The red crystals from the

reaction vessel were of suitable quality for a single-crystal X-ray diffraction analysis.



Characterization data for $[Mo(NO)(Br)_2(dmpe)]_2$. IR (cm^{-1}): 1619 (w, $\nu(NO)$), 1577 (sh, w, $\nu(NO)$). MALDI-TOF (LDI, m/z): 843.7 for $C_{12}H_{32}Br_4Mo_2N_2O_2P_4$ ($[M - NO]^{+}$), 792.7 for $C_{12}H_{32}Br_3Mo_2N_2O_2P_4$ ($[M - Br]^{+}$). HRMS-ESI(+) m/z : ($[M - Br]^{+}$, ^{92}Mo , ^{81}Br) calcd for $C_{12}H_{32}Br_3N_2O_2P_4$ ^{92}Mo , 780.7106; found, 780.7101. 1H NMR (400 MHz, CD_2Cl_2): δ 1.84 (d, $^2J_{HP} = 9.6$, 6H, PMe), 2.06 (d, $^2J_{HP} = 10.8$, 6H, PMe), 2.09–2.25 (m, 4H, PCH_2), 2.34–2.56 (m, 4H, PCH_2). $^{13}C\{^1H\}$ HMBC NMR (100 MHz, CD_2Cl_2): δ 12.8 (m, PMe_3), 17.0 (m, PMe_3), 27.2 (m, PCH_2CH_2P). $^{31}P\{^1H\}$ NMR (162 MHz, CD_2Cl_2): δ 35.4 (s, MoP). Anal. Calcd for $C_{12}H_{32}Br_4N_2O_2P_4Mo_2$: C, 16.53; H, 3.70; N, 3.21. Found: C, 18.75; H, 4.08; N, 3.04. A more satisfactory elemental analysis of the complex has not yet been obtained.



Partial characterization data for Cp^*H : GC-MS m/z (% relative intensity, ion): 136 (95, M^+), 121 (100, $[M - CH_3]^+$), 105 (88, $[M - C_2H_7]^+$), 93 (71, $[M - C_3H_9]^+$), 79 (79, $[M - C_4H_9]^+$). 1H NMR (400 MHz, C_6D_6): δ 0.99 (d, $^3J_{HH} = 7.63$, 3H, CH_3), 1.74 (s, 6H, CH_3), 1.79 (s, 6H, CH_3), 2.42 (q, $^3J_{HH} = 7.63$, 1H, CH). These data match spectroscopic data obtained from an authentic sample of pure Cp^*H in C_6D_6 .

Reaction of $Cp^*Mo(NO)(\kappa^2-dmpe)$ (2) with 1-Bromooctane. In a glovebox, a thick-walled flask was charged with complex 2 (0.101 g, 0.246 mmol) and THF (ca. 10 mL), resulting in a clear bright orange solution. On a double-manifold Schlenk line, 1-bromooctane (0.212 mL, 1.227 mmol) was added into the reaction flask via a micropipette. No color change occurred. The flask was then heated to 70 °C, and the temperature was maintained for 16 h, after which time large dark red crystals had deposited around the sides of the flask, and the supernatant solution had become pale yellow in color. The supernatant solution was decanted from the flask, and the red crystals remaining were washed with THF (3×1 mL) before being dried in vacuo. $[Cp^*Mo(NO)Br_2(\kappa^2-dmpe)]_2$ was collected as a red crystalline solid (0.062 g, 0.071 mmol, 58% yield).

Reaction of $Cp^*Mo(NO)(\kappa^2-dmpe)$ (2) with 5 equiv 1,5-Dibromopentane. In a glovebox, a flask was charged with $Cp^*Mo(NO)(\kappa^2-dmpe)$ (0.102 g, 0.248 mmol) and THF (ca. 8 mL) to obtain a clear, bright orange solution. On a double manifold, 1,5-dibromopentane (0.169 mL, 1.24 mmol) was added to the flask via a micropipette. The stirred contents of the flask were heated at 70 °C for 3 d, whereupon a red, shard-like precipitate deposited on the walls of the flask and the solution lightened to a pale yellow color. The solution was decanted from the flask, and the precipitate was washed with THF until the washes became colorless (5×2 mL). The precipitate was isolated by the removal of solvent in vacuo to obtain complex 6 as a fine red powder (0.081 g, 0.093 mmol, 75% yield). GCMS and 1H NMR spectroscopic analyses of the supernatant solution indicated the presence of Cp^*H , 1-bromopentane, and a bromopentene.

Reaction of $Cp^*Mo(NO)(\kappa^2-dmpe)$ (2) with 1 Equiv of 1,5-Dibromopentane. In a glovebox, a flask was charged with $Cp^*Mo(NO)(\kappa^2-dmpe)$ (0.162 g, 0.393 mmol) and THF (ca. 10 mL) to obtain a clear, bright orange solution. On a double manifold, 1,5-dibromopentane (0.054 mL, 0.39 mmol) was added to the flask via a micropipette. The stirred contents of the flask were heated at 70 °C for 3 d, whereupon the solution turned an opaque brown, and a fine red precipitate of 6 deposited on the walls of the flask. GCMS and 1H NMR spectroscopic analyses of the supernatant solution indicated the presence of 2-pentene and cyclopentene in addition to the products

identified from the reaction of **2** with 5 equiv of 1,5-dibromopentane described in the preceding paragraph.

X-ray Crystallography. Full details of all single-crystal X-ray diffraction analyses are presented in the [Supporting Information](#).

■ ASSOCIATED CONTENT

Supporting Information

The Supporting Information is available free of charge on the ACS Publications website at DOI: [10.1021/acs.inorgchem.7b01733](https://doi.org/10.1021/acs.inorgchem.7b01733).

^1H NMR, $^1\text{H}\{^31\text{P}\}$, and $^31\text{P}\{^1\text{H}\}$ NMR spectra of representative complexes and full details of the single-crystal X-ray diffraction analyses of the reported complexes ([PDF](#))

Accession Codes

CCDC 1559147–1559152 contain the supplementary crystallographic data for this paper. These data can be obtained free of charge via www.ccdc.cam.ac.uk/data_request/cif, by emailing data_request@ccdc.cam.ac.uk, or by contacting The Cambridge Crystallographic Data Centre, 12 Union Road, Cambridge CB2 1EZ, UK; fax: +44 1223 336033.

■ AUTHOR INFORMATION

Corresponding Author

*E-mail: legzdins@chem.ubc.ca.

ORCID

Peter Legzdins: [0000-0002-3914-3768](https://orcid.org/0000-0002-3914-3768)

Notes

The authors declare no competing financial interest.

■ ACKNOWLEDGMENTS

We are grateful to The Dow Chemical Company for financial support of our work and to our Dow colleague Devon Rosenfeld for assistance and helpful comments. We also thank Russell Wakeham, Rex Handford, and Monica Shree for their contributions during the early stages of these investigations and Judy Wrinskelle for her invaluable technical assistance. We are also grateful to the reviewers for their helpful suggestions and comments.

■ REFERENCES

- (1) Baillie, R. A.; Legzdins, P. The Rich and Varied Chemistry of Group 6 Cyclopentadienyl Nitrosyl Complexes. *Coord. Chem. Rev.* **2016**, *309*, 1–20.
- (2) Baillie, R. A.; Legzdins, P. Distinctive Activation and Functionalization of Hydrocarbon C–H Bonds Initiated by $\text{Cp}^*\text{W}(\text{NO})(\eta^3\text{-allyl})(\text{CH}_2\text{CMe}_3)$ Complexes. *Acc. Chem. Res.* **2014**, *47*, 330–340.
- (3) Handford, R. C.; Wakeham, R. J.; Patrick, B. O.; Legzdins, P. Cationic and Neutral $\text{Cp}^*\text{M}(\text{NO})(\kappa^2\text{-Ph}_2\text{PCH}_2\text{CH}_2\text{PPh}_2)$ Complexes of Molybdenum and Tungsten: Lewis-Acid Induced Intramolecular C–H Activation. *Inorg. Chem.* **2017**, *56*, 3612–3622.
- (4) Handford, R. C.; Legzdins, P. Unpublished observations.
- (5) Dryden, N. H.; Legzdins, P.; Batchelor, R. J.; Einstein, F. W. B. Organometallic Nitrosyl Chemistry. 45. Improved Syntheses of Cyclopentadienyl Dichloro Nitrosyl Complexes of Molybdenum and Tungsten. Utility of Phosphorus Pentachloride as a Chlorinating Agent. *Organometallics* **1991**, *10*, 2077–2081.
- (6) Legzdins, P.; Lumb, S. A.; Young, V. G. Ligand Elaboration Mediated by a $\text{Cp}^*\text{W}(\text{NO})$ Template: Stepwise Incorporation of Small Molecules into a Tungsten Vinyl Fragment. *Organometallics* **1998**, *17*, 854–871.
- (7) Such M–S–M linkages are relatively rare. See, for example: (a) Drew, M. G. B.; Mitchell, P. C. H.; Pygall, C. F. Reaction Between

Molybdate(VI), Cyanide, and Hydrogen Sulfide. *Angew. Chem., Int. Ed. Engl.* **1976**, *15*, 784–785. (b) Mealli, C.; Midollini, S.; Sacconi, L. Transition-Metal Complexes with Sulfur Atom as Ligand. 2. Synthesis, Properties, and Structural Characterization of Thio, Mercapto, and Methylthio Complexes of Cobalt(I) and Nickel(I) and – (II) with Poly(tertiary phosphines). *Inorg. Chem.* **1978**, *17*, 632–637. (c) Greenhough, T. J.; Kolthammer, B. W. S.; Legzdins, P.; Trotter, J. Crystal and Molecular Structures of Bis[$(\eta^5\text{-cyclopentadienyl})\text{-dicarbonylchromium}$] Sulfide, a Novel Organometallic Complex Possessing a $\text{Cr}\equiv\text{S}\equiv\text{Cr}$ Linkage. *Inorg. Chem.* **1979**, *18*, 3543–3548.

(8) Huneke, J. T.; Enemark, J. H. The Mo=S Bond Distance in $\text{Di-}\mu\text{-sulfido-bis}[\text{sulfido}(N,N\text{-diethylidithiocarbamate})\text{molybdenum(V)}]$. *Inorg. Chem.* **1978**, *17*, 3698–3699.

(9) Kawaguchi, H.; Yamada, K.; Lang, J.-P.; Tatsumi, K. A New Entry into Molybdenum/Tungsten Sulfur Chemistry: Synthesis and Reactions of Mononuclear Sulfido Complexes of Pentamethylcyclopentadienyl-Molybdenum(VI) and -Tungsten(VI). *J. Am. Chem. Soc.* **1997**, *119*, 10346–10358.

(10) Ito, J.; Ohki, Y.; Iwata, M.; Tatsumi, K. Trithio-Chloro Molybdate $[\text{MoClS}_3]^-$: A Versatile Precursor for Molybdenum Trisulfido Complexes. *Inorg. Chem.* **2008**, *47*, 3763–3771.

(11) Adams, H.; Bancroft, M. N.; Morris, M. J.; Riddiough, A. E. Sequential Construction of One, Two, or Three Dithiolene Ligands from Alkynes and Sulfur in Dinuclear Cyclopentadienyl Molybdenum Complexes. *Inorg. Chem.* **2009**, *48*, 9557–9566.

(12) Lewis, J. Metal-Metal Interaction in Transition-Metal Complexes. *Pure Appl. Chem.* **1965**, *10*, 11–36.

(13) Allen, F. H.; Kennard, O.; Watson, D. G.; Brammer, L.; Orpen, A. G.; Taylor, R. Tables of Bond Lengths Determined by X-Ray and Neutron Diffraction. Part 1. Bond Lengths in Organic Compounds. *J. Chem. Soc., Perkin Trans. 2* **1987**, S1–S19.

(14) Steudel, R. Properties of Sulfur-Sulfur Bonds. *Angew. Chem., Int. Ed. Engl.* **1975**, *14*, 655–664.

(15) Müller, A.; Jaegermann, W.; Enemark, J. H. Disulfur Complexes. *Coord. Chem. Rev.* **1982**, *46*, 245–280 and references cited therein.

(16) This mode of reactivity parallels that recently reported for bis-phosphine palladium precatalysts for which mono-oxidation of the bis-phosphine ligand is critical for the formation of the active catalyst that contains a hemilabile $\kappa^2\text{-P-O}$ ligand. See: Ji, Y.; Plata, R. E.; Regens, C. S.; Hay, M.; Schmidt, M.; Razler, T.; Qiu, Y.; Geng, P.; Hsiao, Y.; Rosner, T.; Eastgate, M. D.; Blackmond, D. G. Mono-Oxidation of Bidentate Bis-phosphines in Catalyst Activation: Kinetic and Mechanistic Studies of a Pd/Xantphos-Catalyzed C–H Functionalization. *J. Am. Chem. Soc.* **2015**, *137*, 13272–13281.

(17) Kochi, J. K.; Powers, J. W. Mechanism of Reduction of Alkyl Halides by Chromium(II) Complexes. Alkylchromium Species as Intermediates. *J. Am. Chem. Soc.* **1970**, *92*, 137–146.

(18) Dykerman, B. A.; Smith, J. J.; McCarvill, E. M.; Gallant, A. J.; Doiron, N. D.; Wagner, B. D.; Jenkins, H. A.; Patrick, B. O.; Smith, K. M. Synthesis of chromium(III) bis(benzamidinate) complexes via single electron oxidation. *J. Organomet. Chem.* **2007**, *692*, 3183–3190.

(19) Poli, R. Relationship between one-electron transition-metal reactivity and radical polymerization processes. *Angew. Chem., Int. Ed.* **2006**, *45*, S058–S070.

(20) Wessjohann, L. A.; Schmidt, G.; Schrekker, H. S. Reaction of secondary and tertiary aliphatic halides with aromatic aldehydes mediated by chromium(II): a selective cross-coupling of alkyl and ketyl radicals. *Tetrahedron* **2008**, *64*, 2134–2142.

(21) Zhou, W.; MacLeod, K. C.; Patrick, B. O.; Smith, K. M. Controlling Secondary Alkyl Radicals: Ligand Effects in Chromium-Catalyzed C–P Bond Formation. *Organometallics* **2012**, *31*, 7324–7327.

(22) Kraatz, H. B.; van der Boom, M. E.; Ben-David, Y.; Milstein, D. Reaction of aryl iodides with (PCP)Pd(II)-alkyl and aryl complexes: Mechanistic aspects of carbon-carbon bond formation. *Isr. J. Chem.* **2001**, *41*, 163–171.

(23) Schwartsburd, L.; Cohen, R.; Konstantinovski, L.; Milstein, D. A pincer-type anionic platinum(0) complex. *Angew. Chem., Int. Ed.* **2008**, *47*, 3603–3606.

- (24) Ji, X. X.; Yang, D. W.; Tong, P.; Li, J. Z.; Wang, B. M.; Qu, J. P. C-H Activation of Cp* Ligand Coordinated to Ruthenium Center: Synthesis and Reactivity of a Thiolate-Bridged Diruthenium Complex Featuring Fulvene-like Cp* Ligand. *Organometallics* **2017**, *36*, 1515–1521.
- (25) Pitman, C. L.; Finster, O. N. L.; Miller, A. J. M. Cyclopentadiene-mediated hydride transfer from rhodium complexes. *Chem. Commun.* **2016**, *52*, 9105–9108.
- (26) Quintana, L. M. A.; Johnson, S. I.; Corona, S. L.; Villatoro, W.; Goddard, W. A.; Takase, M. K.; VanderVelde, D. G.; Winkler, J. R.; Gray, H. B.; Blakemore, J. D. Proton-hydride tautomerism in hydrogen evolution catalysis. *Proc. Natl. Acad. Sci. U. S. A.* **2016**, *113*, 6409–6414.
- (27) Pedersen, A.; Tilset, M. Solvent-Induced Reductive Elimination of Pentamethylcyclopentadiene from a (Pentamethylcyclopentadienyl)metal Hydride. *Organometallics* **1993**, *12*, 3064–3068.
- (28) Jones, W. D.; Kuykendall, V. L.; Selmechzy, A. D. Ring Migration Reactions of $(C_5Me_5)Rh(PMe_3)H_2$ – Evidence for η^3 Slippage and Metal-to-Ring Hydride Migration. *Organometallics* **1991**, *10*, 1577–1586.
- (29) Lewis, J.; Nyholm, R. S. Metal-Metal Bonds in Transition-Metal Complexes. *Sci. Prog. (London)* **1964**, *52*, 557–580.
- (30) Cotton, F. A. *Q. Rev., Chem. Soc.* **1966**, *20*, 389–401.
- (31) Armarego, W. L. F.; Chai, C. L. L. *Purification of Laboratory Chemicals*, 5th ed.; Elsevier: Amsterdam, 2003.
- (32) SDBSWeb. National Institute of Advanced Industrial Science and Technology. <http://sdbas.db.aist.go.jp> (accessed June 8, 2017).